GRID-BASED TACTILE SENSOR SYSTEM FOR SHRINKAGE PRESSURE MEASUREMENT

Perry N. Peralta†

Assistant Professor

and

Audimar P. Bangi†

Researcher
Department of Wood and Paper Science
North Carolina State University
Raleigh, NC 27695-8005

ABSTRACT

A study was conducted to determine the applicability of a grid-based tactile pressure sensor system in monitoring the shrinkage pressure in wood during drying. The sensor was attached to green red oak (*Quercus* sp.) and loblolly pine (*Pinus taeda* L.) boards through a mortise fitted with a two-piece metal insert. As current sensor models could not withstand actual kiln-drying temperatures, the boards were allowed to dry under room conditions (70°F and 60% RH).

Results indicate that the pressure sensor system could accurately monitor the shrinkage pressure within the sample boards. Frame-by-frame recordings of the pressure profile across the loaded sensor grids showed not only a visual manifestation of the stress development and reversal phenomena in drying, but also the magnitudes of the internal compressive stresses. For the first time, both real-time visual graphics and quantitative data on compressive drying stresses in wood are made available. The current sensor system is designed exclusively for measuring compressive stresses, and is incapable of monitoring the magnitude of the internal tensile stresses that occur simultaneously with the compressive stresses.

Keywords: Drying stresses, shrinkage pressure, casehardening, sensor, red oak, loblolly pine.

INTRODUCTION

It has been recognized for many years that the key to the improvement of drying quality and the reduction of drying time lies in the proper understanding and control of internal drying stresses. Experimental studies performed in the past to determine stress distribution within wood during drying relied on a destructive "slicing technique" to relate the observed tensile and compressive strains with the drying stresses in the material (McMillen 1955, 1956, 1963). These studies led to a qualitative establishment of the general stress pattern but failed to provide a more direct, quantitative means of determining drying stresses in lumber. Currently, for lack of precise methods, dry kiln operators have to depend on kiln samples to monitor the lumber's average moisture content to which the stress pattern is related. Interestingly, current technological advances in other fields that deal with the quantitation of stress and strain in materials could potentially change this situation in the future. Of particular significance are the on-going studies on the application of tactile pressure sensors to measure pressure distribution in contacting surfaces.

This study was conducted to evaluate the applicability of a grid-based tactile pressure sensor system in monitoring the shrinkage pressure in wood during drying. The ultimate goal was to develop a quantitative, real-time measurement of stresses in wood during the

† Member of SWST.

drying process. If found feasible, the system could lead to the development of a reliable process control tool that may enable kiln operators to judiciously adjust the dry- and wet-bulb kiln temperatures to bring about drying at the fastest rate possible with little or no defects.

THEORETICAL CONSIDERATIONS

The experimental technique that led to our present-day understanding of drying stresses could be traced to a series of studies performed at the U.S. Forest Products Laboratory (Peck 1940). The so-called "wafer-slicing technique" was used extensively by McMillen (1955, 1956, 1963) in a comprehensive research program on the drying of red oak. It was also employed by Rice and Youngs (1990) to study the rheological behavior of wood during drying. An alternative approach proposed in this study to monitor drying stresses involves the measurement of the shrinkage pressure of wood. While the opposite phenomenon, swelling pressure, has been extensively studied in the past (Barkas 1949; Tarkow and Turner 1958; Simpson and Skaar 1968), there is no existing information in the literature concerning pressure exerted by wood during the process of shrinkage. The principle behind swelling pressure is based on the fact that when wood takes up water, it swells to an extent that depends on the conditions under which the water is adsorbed. One would expect that wood restrained from swelling should exert a pressure in the direction in which it is restrained. This is analogous to the pressure exerted by an osmotic solution against a restraining piston (Skaar 1972). In fact the mathematical expression describing swelling pressure is derived from a generalized osmotic pressure equation that has been modified to account for the gel-like properties of wood (Skaar 1988). In like manner, wood restrained from shrinking should exert a pressure in the direction in which it is restrained. Thus, if a cylindrical hole is drilled normal to the drying wood surface and a metal cylinder

is inserted into the hole, a pressure should be exerted against this metal cylinder as the wood dries and shrinks. The pressure will vary from the surface to the mid-thickness at various stages of drying. The pattern of pressure variation should be similar to the stress pattern that develops during drying. If a correlation could be established between these two parameters, a measurement technique could be developed that will help the kiln operator monitor the drying stresses that arise.

Tactile pressure sensing technology is an innovation in monitoring pressure variations in contacting materials that may prove useful to kiln operators. Despite some initial failures, this technology is showing new promise with the development of grid-based tactile sensor models. These grid-based tactile sensors were first developed in response to a specific need by dentists—that of reliably determining how much pressure is generated when a patient's teeth are contacting. The ultra-thin (0.004 to 0.10 mm) sensor for the tactile pressure measurement system is made up of rows and columns of conductive material deposited onto a thin polyester or polyimide film substrate (Fig. 1). The intersections of the rows and columns sandwich a semiconductive ink whose electrical resistance changes with applied force. By electronically scanning and measuring each point of contact, a given intersection point becomes an independent sensing element. A sensor with a pressure measurement area of 30 cm² typically has 1,936 individual sensing elements, with each element capable of measuring pressures as high as 175 MPa. The sensor connects to a handle that processes the sensor output in a form that can be sent to the computer via a shielded cable connected to an installed data acquisition board. This interface board brings the sensor data into the desktop PC for processing by a specially designed software component.

Today, these sensors are not only used worldwide in the biomedical profession, but are also increasingly gaining acceptance in a multitude of industrial applications. Their
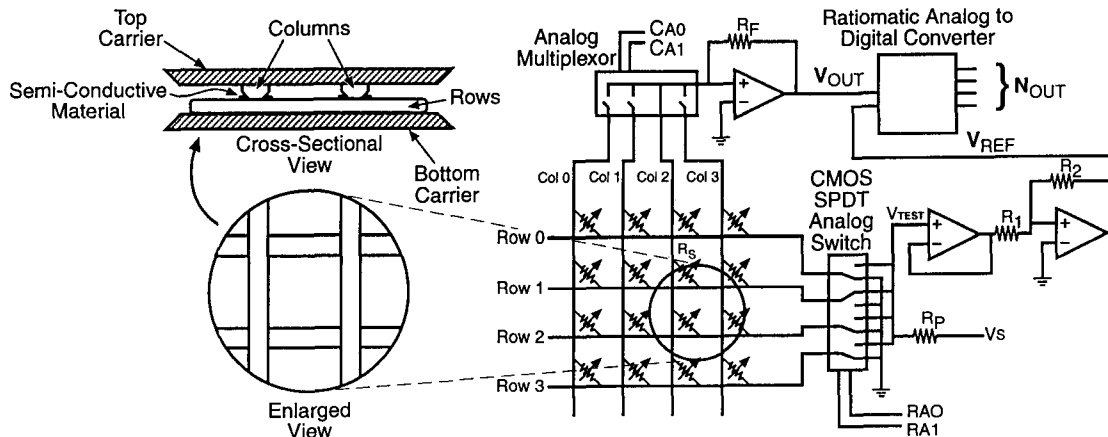
FIG. 1.   Schematic diagram of the grid-based tactile pressure sensor system.

easy-to-use, reliable, and extremely cost-effective features all account for their popularity.

MATERIALS AND METHODS

Sample boards

Freshly-cut 2.5-cm-thick by 14.0-cm-wide red oak (*Quercus* sp.) and 2.5-cm-thick by 10.2-cm-wide loblolly pine (*Pinus taeda* L.) lumber were obtained from a sawmill in Smithfield, North Carolina. Two 30-cm-long sample boards were cut from each species and then end-coated. Moisture sections were also taken from the lumber to determine their green moisture contents.

Tactile sensor specifications

Two sensor models were used in the study: one, with a pressure range of 0 to 69 MPa, was used for the red oak sample; and another, with a pressure range of 0 to 34 MPa, was used for the pine sample. Both sensor models can be used within the temperature range from 0 to 49°C, beyond which their accuracy or stability deteriorates.

Sensor conditioning, equilibration, and calibration

Sensor conditioning, equilibration, and calibration were performed in a Tinius Olsen Universal Testing Machine. It is recommended that the sensors be conditioned (or "exercised") prior to calibration to ensure that they respond uniformly to repeatedly applied loads. Conditioning was performed by loading the sensors three to five times, gradually to pressures of approximately 80% of the maximum sensor capacity.

To minimize the inherent variations between individual sensing elements, the sensors were also subjected to equilibration prior to calibration by applying a relatively uniform pressure. This was accomplished by inserting the sensor and a thin paperboard between two rigid reaction plates and then applying compression load to the assembly using the testing machine. The paperboard served to even out the pressure applied on the sensor and roughly simulates a fibrous wooden surface in the actual testing. While on load, the software performs internal adjustments so that each element within the sensor would produce a reasonably uniform output.

After conditioning and equilibration, the sensors were calibrated in accordance with the instrument manufacturer's recommended 2-point calibration scheme, in which two different known and uniform loads were applied to the sensor. The instrumentation software then performed a power law interpolation based on zero load and the two known calibration loads. The calibration process translates the electrical
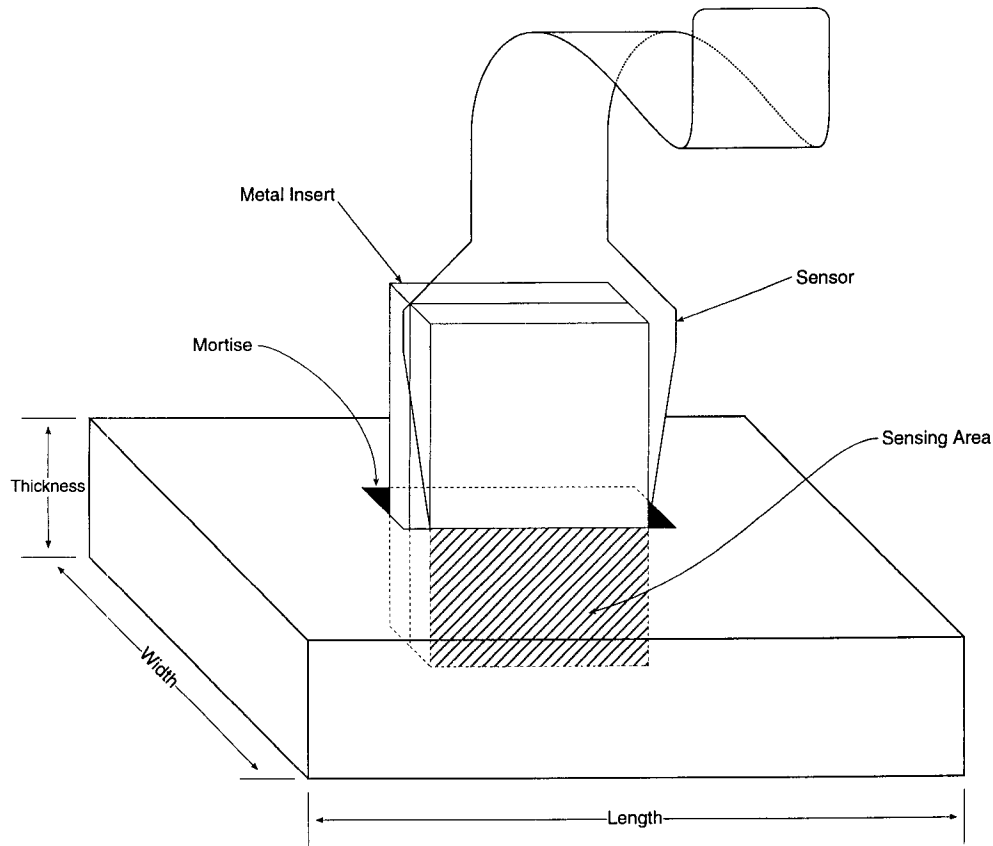
FIG. 2.   Schematic diagram showing the position of the tactile sensor and the two-piece metal inserts relative to the sample board.

resistance signals from the sensors into a measurement (force or pressure) unit.

Drift in sensor output

The change in sensor output when subjected to a constant load input over a period of time was monitored by using specially selected weights. Drift is influenced by such factors as sensor design, sensor sensitivity, the applied load, and environmental conditions.

Sensor installation in the board

A 9.75-mm by 82.55-mm rectangular hole perpendicular to the wide surface was drilled on the center of the board using a mortiser. The width of the mortise was decided based on the tapered sensor width (Fig. 2), which

was 82.55 mm at the widest point. Two smooth and flat stainless steel inserts each measuring 4.88 mm by 58.42 mm by 63.5 mm were used to fix the sensor in place. The position and placement of the sensor and metal inserts relative to the sample board are shown in Fig. 2.

Monitoring of drying stresses

Because of the temperature sensitivity of the sensors, the boards were allowed to dry under room conditions (70°F and 60% relative humidity). Each board was monitored for internal stresses by recording the pressure exerted by the drying board on the sensor every 24-h interval. The frame-by-frame recordings were stored and saved in disk files.

Early Stages   Middle Stages   Late Stages

(a)

Early Stages   Middle Stages   Late Stages
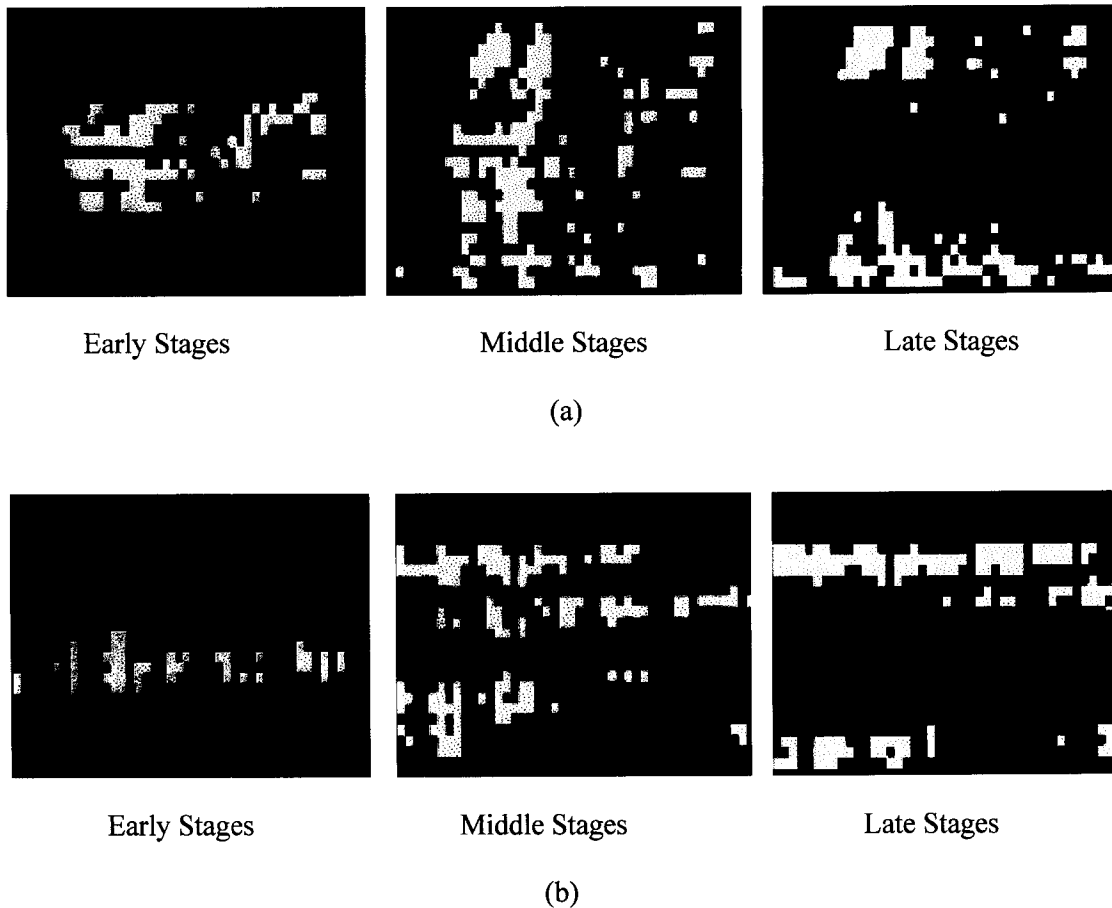
(b)

FIG. 3.   Pressure profiles for (a) loblolly pine and (b) red oak, during the early, middle, and late stages of drying. Darker shades of gray represent lower pressures, while increasingly lighter shades represent higher pressures.

At the end of drying, 2.5-cm-wide sections were taken about 2.5 cm away from both ends of the sample boards for postdrying stress evaluation. Following the method used by McMillen (Rice and Youngs 1990), each section was weighed and then measured for pre-cut length (oriented along the width of the board). Each stress section was immediately cut into five slices using a small bandsaw. Each slice was weighed and then measured for postcut length.

RESULTS AND DISCUSSION

The performance of the sensors in terms of their ability to monitor the instantaneous shrinkage pressure distribution within the sam-ple boards can be inferred from the pressure profile recordings for the initial, middle, and end stages of drying for pine (Fig. 3a) and oak (Fig. 3b). These graphs display the pressure range for each sensing element through 13 pressure ranges, represented by dark-to-light shades of gray. Lower pressures are represented by darker shades, while progressively increasing pressures are represented by increasingly lighter shades. Both the pressure profile and the numerical value of pressure at each sensing element are acquired in real-time at frequencies as high as 126 Hz. The acquired data can later on be replayed and stopped at any desired frame. The frames in Fig. 3a are just three of the 36 frames acquired during the

18-day drying of loblolly pine. Those in Fig. 3b are representative of 60 frames acquired during 30 days of oak drying. A graph of pressure versus time at any of the sensing elements can also be generated, allowing for detailed analysis of pressure distribution.

The pressure profiles (Fig. 3) manifest a well-known theoretical pattern of internal stress development during wood drying. As can be noted in both wood species, the wood core is subjected to high shrinkage pressure (compressive stress) during the early stages of drying, as manifested by the centralized location of the lighter-colored sensing elements in the first frame. As drying progresses, the shrinkage pressure distribution moves out towards the board surfaces such that at the middle stage (second frame) the pressure evens out across the thickness of the board. Towards the later stages of drying (third frame), the shrinkage pressure within the core disappears, while the outer shells are now under high shrinkage pressure. During this period, the internal stresses have reversed and the core is believed to be under tension and the shell under compression, that is, the board is in a case-hardened state. One interesting aspect of the pressure profile recordings needs to be noted here. As can be seen from the frame-by-frame recordings for red oak, the stress pattern across the thickness of the board is skewed toward one side, which visually depicts a board undergoing asymmetrical shrinkage (cupping).

A plot of internal shrinkage pressure versus drying time for two sensing elements (one at the shell, the other at the core) is shown in Fig. 4a and 4b for pine and red oak, respectively. In both figures, the moisture content curve is also superimposed on the shrinkage pressure curves. For loblolly pine (Fig. 4a), the stainless steel inserts were tightly fitted in the mortise during installation such that an average initial pressure of 530 KPa was recorded. The pressure curve for pine shows that the shrinkage pressure at the shell relaxed from 530 KPa at the start of drying when the average moisture content was 130% to 0 KPa at

the fourth day of drying when the average moisture content was 28%. The measurement system cannot measure negative pressure, thus the pressure curve for pine remained at 0 KPa during days 4 to 6. By using the 530 KPa level as the baseline, pressure readings from day 2 to day 7 can be viewed as negative and hence indicate that the shell was being subjected to tensile stress. It is conceivable that if the initial pressure were higher than 530 KPa, the curve would have dipped further, maybe showing a minimum on the fifth day of drying when the average moisture content was 22%. The ninth day of drying (average MC = 13%) shows a pressure level at the shell higher than the initial pressure, indicating stress reversal, that is, the shell is now under compression. The pressure curve rises steeply until it levels off starting on the 12th day. The core of loblolly pine was subjected to appreciable compressive stress roughly between the third and the 11th day of drying, reaching a maximum on the 7th day of drying when the average moisture content was 16%. The pressure at the core goes to near 0 KPa on the 12th day (average MC = 11%), signaling the start of stress reversal. Pressure remained at this level until the end of the drying process. From theory, the core should be under tensile stress during this period. This stress is not reflected here because the system cannot measure negative pressure.

For red oak (Fig. 4b), the stainless steel inserts were not tightly fitted in the mortise during installation. This has something to do with the difficulty of cutting this species and the variability inherent in any machining operation. Thus, the shrinkage pressure at the shell remained at 0 KPa from the start of the experiment when the average moisture content was 86% until the 12th day of drying when the average moisture content was 33%. The shrinkage pressure at the shell of red oak started to increase on the 13th day (average MC = 31%), indicating stress reversal. This compressive stress continued to go up until the end of the drying period. Just as in loblolly pine, the core of red oak was under compressive stress starting on the third day when the av-
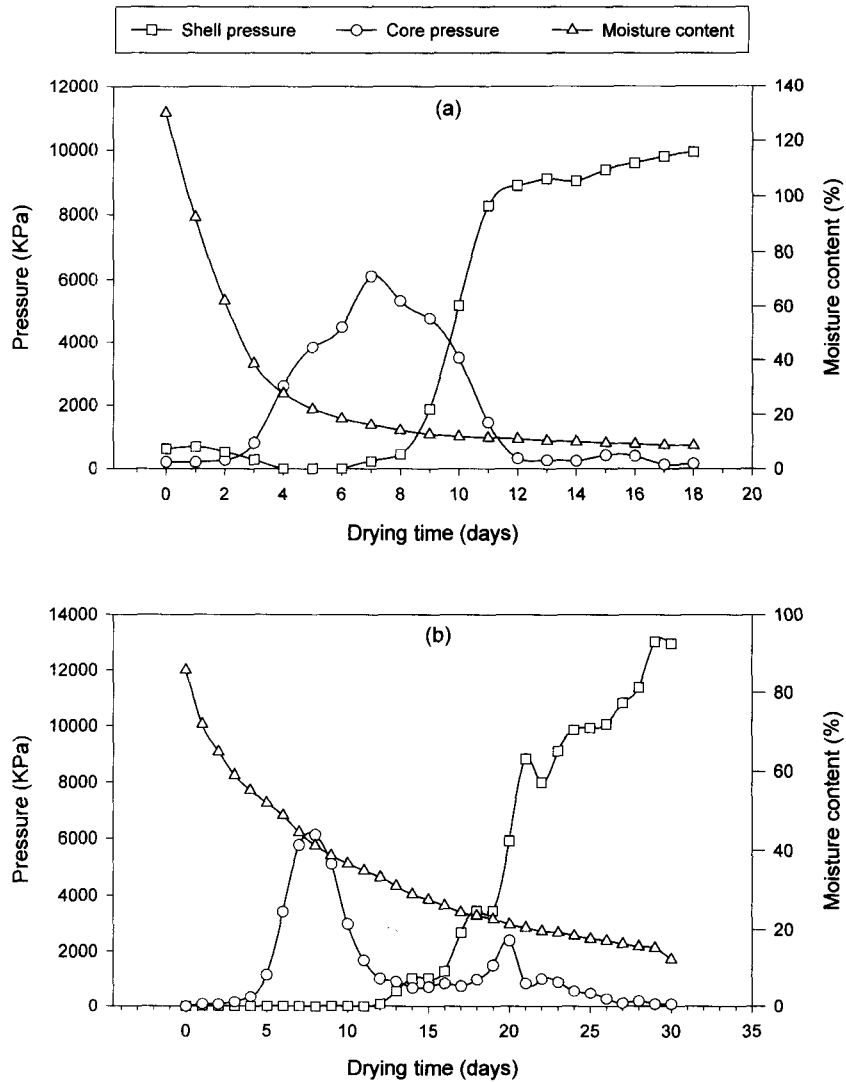
Fig. 4. Plot of shrinkage pressures at the shell and core versus drying time for (a) loblolly pine and (b) red oak, superimposed on the moisture content curve.

erage moisture content was 59%, reached maximum on the 8th day (average MC = 41%), decreased and remained at around 0 KPa from the 13th day (average MC = 31%) until the end of the drying process.

An examination of the stress sections for four replicates of loblolly pine indicates that at the end of drying, when the moisture content has dropped to 8%, the outer shells tend to elongate after slicing (Fig. 5), confirming

that these zones were under compressive stress prior to slicing. In contrast, the core and intermediate slices showed a general tendency to contract after slicing, which indicates that these zones were under tension prior to slicing. However, as mentioned earlier, the tactile pressure sensor system being tested does not provide any quantitative proof for the latter. The inability of the measurement system to show negative pressure is a major inadequacy
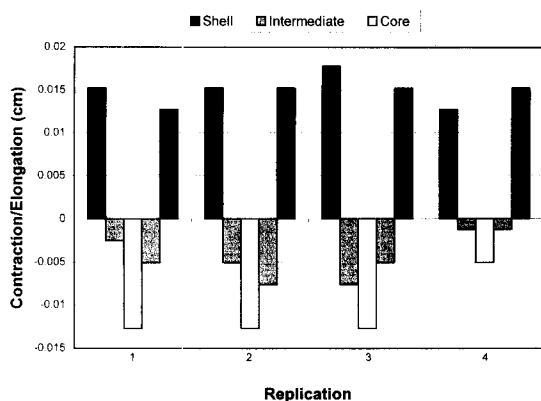
Fig. 5.   Contraction/elongation diagram of the shell, core, and intermediate slices for four replicates of loblolly pine evaluated for drying stress using the slicing method.
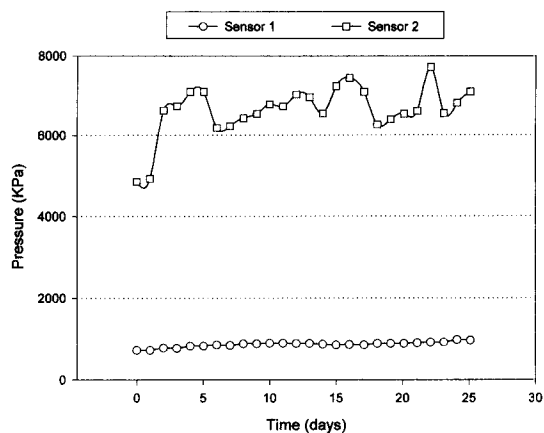

Fig. 6.   Graph showing the drift pattern in the control sensors subjected to constant pressure of 730 KPa (Sensor 1) and 4,800 KPa (Sensor 2).

since indication of tensile stress is critical in controlling tension-induced defects like checking and honeycombing.

It should be pointed out here that the preceding results were not corrected for any drift in sensor output. Two control sensors that were subjected to constant loads to specifically monitor the change in sensor output as a function of time show that at the lower pressure (730 KPa), the output (Sensor 1, Fig. 6) remained more or less stable. However, the sensor loaded at a higher pressure (4,800 KPa) showed a significant increase in sensor output and considerable output fluctuations (Sensor 2, Fig. 6).

CONCLUSIONS AND RECOMMENDATIONS

In conclusion, this study has provided some insights into the potential use of grid-based tactile pressure system for monitoring shrinkage pressure in wood during drying. The observed ability of the sensors to monitor the stress development and reversal phenomena in lumber drying is very encouraging, but future studies need to improve on the measurement system and procedures.

For future follow-up studies, a number of key technical issues need to be addressed, as follows:

(1) Development of a sensor that is accurate and stable under high temperature condi-

tions. This sensor improvement is critical if the measurement system has to find application in commercial lumber drying. Current sensor models are sensitive to elevated temperatures, especially above 49°C. According to the manufacturer, the sensor may be operable up to 95°C, but a temperature correction factor remains to be established; above 120°C, the sensor's functionality becomes irrecoverable (McWilliams 1998).

(2) Design of a better sensor insertion mechanism that would allow the initial pressure on the sensors at the start of drying to be adjustable. This need stems from the fact that cutting the mortise involves some mortise width variability resulting in tightly fit metal insert in some samples and loosely fit metal insert in other samples. Slightly tapered twin-metal inserts with a special locking mechanism may be appropriate in this case.

(3) Investigate the effect of board width, the size of the mortise slot, and the rigid nature of the metal inserts on stress development in the sample boards, especially within the vicinity of the sensor-wood-insert contact area.

REFERENCES

BARKAS, W. W. 1949. Swelling of wood under stress. Department of Scientific and Industrial Research, London, UK. 103 pp.
McMILLEN, J. M. 1955. Drying stresses in red oak. Forest Prod. J. 5(1):71–76.
————. 1956. Drying stresses in red oak: effect of temperature. Forest Prod. J. 5(4):230–241.
————. 1963. Stresses in wood during drying. USDA Forest Service Report No. 1652. Forest Prod. Lab., Madison, WI. 52 pp.
McWILLIAMS, C. 1998. Personal communication. Tekscan, Inc., Boston, MA 02127-1342.
PECK, E. C. 1940. A new approach to the formulation of hardwood dry-kiln schedules. Southern Lumberman 161(2033):136–137.
RICE, R. W., AND R. L. YOUNGS. 1990. The mechanism and development of creep during drying of red oak. Holz Roh- Werkst. 48:73–79.
SIMPSON, W. T. (ed.). 1991. Dry kiln operator's manual. Agriculture Handbook No. 188. USDA Forest Service, Forest Prod. Lab., Madison, WI. 274 pp.
————, AND C. SKAAR. 1968. Effect of restrained swelling on wood moisture content. USDA Forest Service Research Note FPL-0196.
SKAAR, C. 1972. Water in wood. Syracuse University Press, Syracuse, NY. 218 pp.
————. 1988. Wood-water relations. Springer-Verlag, Berlin, Germany. 283 pp.
TARKOW, H., AND H. D. TURNER. 1958. The swelling pressure of wood. Forest Prod. J. 8:193–197.